Submitted to Environmental Earth Sciences: NovCare 2015 Thematic Issue

Comparison of slug and pumping tests for hydraulic tomography experiments: A practical perspective

Daniel Paradis[1], René Lefebvre[2], Erwan Gloaguen[2], and Bernard Giroux[2]

1: Geological Survey of Canada, 490 rue de la Couronne, Quebec City, Canada G1K 9A9
2: Institut national de la recherche scientifique, Centre Eau Terre Environnement (INRS-ETE), 490 rue de la Couronne, Quebec City, Canada G1K 9A9

Corresponding author: Daniel Paradis
Phone: (418) 654-3713 Fax: (418) 654-2604 E-mail: daniel.paradis@canada.ca

KEYWORDS: Aquifer characterization, Heterogeneity, Hydraulic tomography, Slug tests, Pumping tests, Resolution analysis, Principle of reciprocity

ABSTRACT

Hydraulic tomography is the simultaneous analysis of several hydraulic tests performed in multiple isolated intervals in adjacent wells to image heterogeneous hydraulic property fields. In this study, we compare the resolutions associated with hydraulic tomography experiments carried out with slug tests and pumping tests for simple configurations with hydraulic property values representative of an extensively studied littoral aquifer. Associated test designs (e.g., pumping rates, test durations) and the validity of the principle of reciprocity are also assessed. For this purpose, synthetic tomography experiments and their associated sensitivity matrices are generated using a radial flow model accounting for wellbore storage. The resolution analysis is based on a pseudo-inverse analysis of the sensitivity matrix with a noise level representative of field measurements. Synthetic experiments used equivalent perturbations for slug tests and pumping tests. Even though pumping tests induce a drawdown in observation intervals that is three times larger than head changes due to slug tests, resolutions for hydraulic conductivities (horizontal and vertical) are similar for the two tests and slightly lower for specific storage with pumping. However, experiments with pumping require fifty times more water and are seven times longer to perform than experiments with slug tests. Furthermore, reducing pumping rates to limit disposal of water or test durations to decrease field data acquisition time would considerably lower resolutions for either scenario. Analyses are done using all available stressed and observation intervals as required by the non-applicability of the principle of reciprocity for slug tests and pumping tests with important wellbore storage. This study demonstrates concepts that have important implications for the performance and analysis of hydraulic tomography experiments.

1 Introduction

Knowledge of the hydraulic heterogeneity that controls flow and transport in aquifer systems, such as preferential flow paths and impermeable barriers, is essential for sound groundwater resource protection. Slug tests and pumping tests are common field experiments used to estimate the hydraulic properties of aquifer systems (Kruseman and de Ridder, 2000). A slug test consists of inducing an instantaneous change in water level in a well, whereas a pumping test involves withdrawing water out of a well at a controlled, generally constant, rate. For both kinds of hydraulic tests, water level response is measured in one or more surrounding observation wells and in the stressed well itself. The area affected by a hydraulic test is a function of the hydraulic diffusivity defined by the ratio of hydraulic conductivity (*K*) and specific storage (S_s). The larger the hydraulic diffusivity, the larger will be the response in the observation well and the farther from the stressed well will it be possible to measure the response with a good signal to noise ratio . Several authors have proposed the use of hydraulic tomography to define heterogeneous hydraulic property fields (e.g., Tosaka et al., 1993; Gottlieb and Dietrich, 1995; Butler et al., 1999; Yeh and Liu, 2000; Bohling et al., 2002; 2007; Brauchler et al., 2003, 2010, 2011, 2013; Zhu and Yeh, 2005; Illman et al., 2007, 2008; Fienen et al., 2008; Cardiff et al., 2009; Illman et al., 2009; Berg and Illman, 2011, 2013, 2015; Cardiff and Barrash, 2011; Huang et al., 2011; Cardiff et al., 2012; Sun et al., 2013; Paradis et al., 2015; 2016). Hydraulic tomography is the simultaneous analysis of several hydraulic tests performed in multiple wells or multiple isolated intervals in wells, which provides a better resolution capability of hydraulic property fields than conventional hydraulic tests (Butler, 2005). Analysis of hydraulic tomography data is essentially related to inverse problems with issues related to non-uniqueness of the solution as the number of unknown parameters is usually greater than the number of measurements (under-determined problem) or the data do not contain enough information about the model parameters (rank-deficient problem) due to the physics of the problem and experimental configuration (e.g., Carrera and Neuman, 1986; Yeh and Liu, 2000; Tonkin and Doherty, 2005; Illman et al., 2008; Bohling, 2009; Xiang et al., 2009; Bohling and Butler, 2010; Huang et al., 2011; Liu and Kitanidis, 2011; Paradis et al., 2015, 2016). While regularization for constraining the number of possible solutions is an important topic (e.g., Tikhonov, 1963; Tikhonov and Arsenin, 1977; Kitanidis, 1995; Vasco et al., 1997; Carrera and Neuman, 1986; Yeh and Liu, 2000; Doherty, 2003; Caers, 2005; Rubin and Hubbard, 2005; Tonkin and Doherty, 2005; Carrera et al., 2005; Fienen et al., 2008; Illman et al., 2008; Berg and Illman, 2011; Cardiff and Barrash, 2011; Huang et al., 2011; Cardiff et al., 2012; Sun et al., 2013; Soueid Ahmed et al., 2014; Zha et al., 2014), this paper focuses rather on some practical aspects related to hydraulic tomography, which is of crucial importance to guide practitioners involved in hydraulic property characterization either in terms of estimates accuracy or field efficiency.

The ability of a hydraulic experiment to resolve hydraulic property fields from observations can be understood through the analysis of the sensitivity of head or drawdown to the parameters associated with the aquifer system to characterize (Menke, 1989; Aster, 2005). Sensitivity magnitudes and correlations indicate which parameters can be better resolved. For example, it has been recognized by Butler and McElwee (1990) that varying the magnitude and frequency of the pumping rate scheme of a pumping test can increase parameter resolutions by increasing sensitivity magnitudes while simultaneously constraining sensitivity correlations. While constant rate pumping tests are the most used tests for hydraulic tomography (see the comprehensive summary of previously published studies dedicated to hydraulic tomography provided by Cardiff and Barrash, 2011), few efforts have been dedicated to understanding the impact of test initiation methods on the resolution of hydraulic property fields. Actually, since slug and pumping tests generate very different hydraulic perturbations, it would be worth assessing whether those tests produce different parameter resolution characteristics for hydraulic tomography experiments. Indeed, early times hydraulic response for a pumping test is known to be mostly sensitive to parameters between the stressed and observation wells, whereas the relative influence of parameters outside the inter-well region increases as the drawdown spreads away from the observation well (Oliver, 1993; Leven et al., 2006). On the other hand, it is generally considered that only the immediate vicinity of the stressed well can be resolved with a slug test because the change in hydraulic head pulse is sharply vanishing away from the stressed well (Ferris and Knowles, 1963; Rovey and Cherkauer, 1995).

The main objective of this study is then to compare the resolutions associated with tomography experiments carried out with slug tests and pumping tests. In particular, we are interested by the resolution of horizontal hydraulic conductivity (K_h), K anisotropy (ratio of vertical and horizontal

K, K_v/K_h), and S_s. Moreover, choices in hydraulic test design (e.g., test stress: pumping rate and initial head, test duration) are often made to get around some technical difficulties often encountered during field tomography experiments, such as desaturation of the stressed interval, noisy measurements and excessive test durations. Thus, in an effort to maximize the quality of the information contained in field data, often-acquired at large expenses, we also assess the impact of some field practices associated to the realization of hydraulic tests and verify the validity of the principle of reciprocity for both kinds of tests.

After presenting the general approach followed to evaluate the resolution matrix of a tomography experiment in Section 2, we verify the applicability of the principle of reciprocity for slug and pumping tests and we discuss the implications for acquisition and analysis of tomography data in Section 3. Then, Section 4 presents a comparison of resolution for tomography experiments using slug tests and pumping tests as well as the impact of reduced test stresses (pumping rates and initial heads) and test durations. Finally, we summarize and discuss the main findings of this study in Section 5.

2 General approach for the evaluation of the resolution matrix

The observations (head or drawdown) made during a hydraulic test are sensitive to the hydraulic properties or parameters of the aquifer system at locations reached by the perturbation induced by the test (Vasco et al., 1997). Parameter sensitivity is the ratio of the change in the observations to a unit relative change in a parameter value. The relative magnitude of the sensitivity for different parameters indicates which parameters can be better resolved from the observations. Also, parameters that have dissimilar (non-correlated) temporal sensitivity patterns throughout a test can be resolved separately because they have different effects on observations. A resolution matrix combines sensitivities from a number of observations and for a number of parameters into a single measure related to each parameter, which integrates the effects of sensitivity magnitudes and correlations, and that can be analyzed to assess the ability to resolve parameters from tomography experiments. Figure 1 illustrates the general approach followed to evaluate the resolution matrix of a tomography experiment carried out with slug tests or pumping tests. Further details about this approach proposed by Clemo et al. (2003) that is summarized below can be found in Bohling (2009) and Paradis et al. (2015).

1. Forward modeling and sensitivity calculation. To simulate hydraulic tests (slug and pumping tests) and to compute sensitivities of the synthetic tomography experiments, we used the numerical simulator lr2dinv (Bohling and Butler, 2001). This simulator is a two-dimensional (2D) axisymmetric finite-difference model that describes flow to a partially penetrating well in response to an instantaneous change in water level (e.g., slug test) or to a pumping stress in a confined aquifer through the radial groundwater flow equation. The simulator also allows the explicit simulation of wellbore storage effects and placement of packer intervals in the stressed well.

Using lr2dinv, the sensitivity matrix elements are constructed by a sequence of groundwater flow simulations, one simulation per parameter grid cell, in which each hydraulic property in a single cell is slightly perturbed (1%) from its original value and the differences in head or drawdown are noted. Each $J_{m,n}$ element in the sensitivity matrix represents the normalized sensitivity of the head or drawdown at a given time and location, h_m, to one of the model parameter, p_n:

$$\mathbf{J} = J_{m,n} = p_n \frac{\partial h_m}{\partial p_n} \qquad (1)$$

The head or drawdown index m runs over all observation times and locations for all simulated tests, and p_n represents either the K_h, K_v/K_h or S_s value associated with each cell in the parameter grid. It should be noted that groundwater flow associated with each tomography experiment is nonlinear, and we thus assume that the sensitivity matrix with its elements given by (1) provides a close approximation of the behavior of the nonlinear flow in the vicinity of the model parameters used for each synthetic simulations given the fact that small perturbations are used to compute sensitivities (Bohling, 2009). Details about mathematical formulation and numerical implementation can be found in Bohling and Butler (2001) and Butler and McElwee (1995).

For all synthetic simulations, we use a 2D simulation grid with 43 cells of logarithmically increasing dimension along the radial axis encompassing the stressed and observation wells and 26 cells of dimension equal to 0.3048 m (1 foot) along the vertical axis. This discretization places the zero-head outer boundary of the model very far from the stressed well (about 111 m), so that it has negligible effects on simulated heads or drawdown at the stressed and observation wells. Confined conditions are also assumed to define lower and upper boundary conditions. Slug tests are simulated by modifying the initial head condition at the cells representing the stressed interval, with all other heads in the model set to zero, in order to produce an instantaneous head perturbation into the aquifer. And, pumping tests are simulated through the boundary condition by specifying the pumping rate in the stressed interval. Note that to avoid desaturation of the stressed interval (water level below the top of the screen) slug tests and pumping tests are simulated by injecting water into the synthetic aquifer. Specific parameter grid discretization and parameter values for each synthetic experiment discussed in this study are presented later in their respective section.

2. Moore-Penrose pseudo-inverse and resolution matrix. Given a vector **m** of *n* parameters to be estimated, the Moore-Penrose pseudo-inverse $\mathbf{J}_p^{\dagger}$ (Moore, 1920; Penrose, 1955) can be used in computing a least-squares and minimum length solution $\mathbf{m}_{\dagger}$ from a data vector **d** of *m* observations (head or drawdown) as (Menke, 1989; Aster, 2005):

$$\mathbf{m}_{\dagger} = \mathbf{J}_{\mathbf{p}}^{\dagger}\mathbf{d} \tag{2}$$

where $\mathbf{J}_p^{\dagger}$ is the sensitivity matrix **J** retaining the *p* largest singular values and vectors of its singular value decomposition corresponding to the most strongly resolved parameters. Note that the Moore-Penrose pseudo-inverse is a convenient way of analyzing the information content of least-squares inverse problems (e.g., Bohling, 2009; Paradis et al, 2015) without having to optimize an objective function that could be computationally intensive. If the true model of parameters are represented by the vector **m** and the corresponding true data vector is represented by **d**=**Jm**, then the estimated parameter vector from the pseudo-inverse $\mathbf{m}_{\dagger}$ can be expressed from (2) as (Menke, 1989; Aster, 2005):

$$\mathbf{m}_{\dagger} = \mathbf{J}_{\mathbf{p}}^{\dagger}\mathbf{J}\mathbf{m} = \mathbf{R}\mathbf{m} \tag{3}$$

The matrix multiplying the true model of parameters **m** is called the resolution matrix:

$$\mathbf{R} = \mathbf{J}_\mathbf{p}^{\dagger}\mathbf{J} \quad (4)$$

where the elements of **R** are indicators of the relative magnitude and correlation between parameter sensitivities resulting from the pseudo-inverse. For this study, only the diagonal elements of **R** that indicate the resolution of each parameter are analyzed. The values of diagonal elements are between 0 and 1: a value of 0 means that a parameter cannot be resolved from the observations, whereas a value of 1 means it can be perfectly resolved. Discussion about the information contained in the entire resolution matrix can be found in Menke (1989) and Aster (2005).

To get a common basis of comparison among the different tomography experiments using slug tests and pumping tests, we select for each experiment the number of *p* singular values and vectors in (4) according to a predefined level of error in parameter estimates resulting from the pseudo-inverse. As proposed by Clemo et al. (2003), *p* can indeed be selected by considering **d** in (2) as the random noise in the observations $\boldsymbol{\eta}$ and **m** as the error in the parameter estimates $\Delta\mathbf{m}_\dagger$, which leads to the following:

$$\Delta\mathbf{m}_\dagger = \mathbf{J}_\mathbf{p}^{\dagger}\boldsymbol{\eta} \quad (5)$$

Thus, for a given level of parameter error, defined here as the root-mean-square of the norm of $\Delta\mathbf{m}_\dagger$, the number of *p* singular values and vectors to retain for the evaluation of the resolution matrix in (4) is selected using (5) (see Bohling, 2009). For this study, we choose an error $\Delta\mathbf{m}_\dagger$ of 0.1 (average relative error of 10%) and define a Gaussian noise $\boldsymbol{\eta}$ (mean of zero; standard deviation of $2\text{x}10^{-4}$ m) realistic of field experimentations (e.g., Bohling, 2009; Paradis et al., 2015).

Figure 1

3 Verification of the principle of reciprocity

In this section, we investigate the applicability of the principle of reciprocity for slug tests and pumping tests as it may have implications for the acquisition and analysis of tomographic data, and consequently on parameter resolutions as well. The principle of reciprocity states that, as long as wellbore storage effects can be neglected, reciprocal tests for which the role of the stressed and observation intervals are interchanged produce identical observation interval responses regardless of the degree of heterogeneity (see proof in McKinley et al., 1968). To verify this principle, we simulate head and drawdown for reciprocal tests that are symmetrical (Figure 2a) and asymmetrical (Figure 3a) with respect to the heterogeneity in K_h, K_v and S_s. Thus for both models, reciprocal tests are simulated by varying each hydraulic property of layer 2 one at a time (black layers in Figures 2a and 3a) while holding all other properties unchanged (Table 1). We note also that stressed and observation interval locations in Figures 2a and 3a are symmetrical to the upper and lower no-flow boundaries to avoid misinterpretation of the reciprocal tests. Wellbore storage is also only simulated in the stressed intervals as we assume that wellbore storage effects in straddled observation intervals with packers can be neglected (Sageev, 1986; Novakowski, 1989).

Figures 2b and 2c present results of the reciprocal slug tests and pumping tests, respectively, for the symmetrical cases. Obviously, reciprocal responses are indistinguishable whether the test is initiated in well 1 or well 2 since those tests are performed under identical conditions (note that reciprocal curves are superposed in Figure 2). Figures 3b and 3c show however that for the asymmetrical cases, that the reciprocal head and drawdown responses in the observation intervals are different when K_h and K_v are varied, which refutes the principle of reciprocity.

As suggested by the comparison of Figures 3c and 3d for reciprocal pumping tests considering and neglecting wellbore storage, respectively, the refutation of the principle of reciprocity for observation interval responses could be explained by a wellbore storage effect. Note that stressed interval responses differ regardless of the degree of heterogeneity. In fact, for a pumping test in a well with a large diameter, the total pumping rate (Q) set by the pump is the combined contributions of flow rates coming from the wellbore (Q_w) and the aquifer system (Q_a) (Dougherty and Babu, 1984). Wellbore storage supplies most of the initial pumped water, which initially equals to Q and gradually decreases to zero when pumping continues. In contrast, the contribution from the aquifer system is initially zero and gradually approaches Q when drawdown is reaching steady-state. Also, the relative contributions of Q_w and Q_a that must balance with Q vary according to the hydraulic properties surrounding the stressed well ($Q=Q_a+Q_w$). Note here that we only consider wellbore storage due to water level change and not from water compressibility. Thus, as the drawdown in an observation interval is controlled by the flow at this location Q_{obs}, which depends on Q_a at the stressed interval and the heterogeneity travelled by the hydraulic perturbation, reciprocal drawdown responses in Figure 3c differ because Q_a is different for each reciprocal test while the heterogeneity seen in reverse order by the hydraulic perturbations is the same in the two directions of testing. For pumping tests where wellbore storage can be neglected (Q_w=0), Q_a is independent of the heterogeneity surrounding the stressed well and is equal to the same constant value of Q for the two reciprocal tests ($Q_a=Q$), which explains the identical reciprocal observation interval responses in Figure 3d. We note in Figure 3c that reciprocal observation interval responses are identical at steady-state when wellbore storage effect becomes negligible. Finally, a similar reasoning can be applied for slug tests in Figure 3a where Q_a is proportional to the decline of the water level in the the stressed interval ($Q_a=Q_w$; Q=0), which is also controlled by the hydraulic properties surrounding the stressed interval.

In summary, the principle of reciprocity as applied to observation interval responses is valid for cases where wellbore storage effects can be neglected. This is not the case for slug tests or pumping tests with large diameter boreholes. As a consequence, stressed and observation interval responses must be recorded during field testing and used together in the analysis of hydraulic tomography experiments.

Table 1

Figure 2

Figure 3

4 Comparison of resolutions for different hydraulic test designs

This section explores the effects of different hydraulic test designs used for tomography experiments on parameter resolutions. In particular, we assess the effects of test initiation methods (slug and pumping tests), reduced test stresses (initial heads and pumping rates) and reduced test durations.

4.1 Effect of test initiation methods

In this section, we compare the resolutions of two tomography experiments that use slug tests and pumping tests, respectively. To compare parameter resolutions on a common basis over the domain, we use a parameter grid with similar cell sizes. The simulation grid was thus divided into 143 cells of 0.61 m in height, that corresponds to the length of the stressed interval, and, due the logarithmic change in cell dimensions in the radial direction, the cells of the simulation grid were merged laterally to obtain cell widths of approximately equal size (Figures 4a and 4b). Sensitivities for the resolution analysis are also computed from a homogeneous and anisotropic model with bulk average K_h, K_v/K_h and S_s values of 1×10^{-5} ms^{-1}, 0.1 and 1×10^{-5} m^{-1}, respectively. Those values are representative of the hydrogeological conditions present at the St-Lambert site in Canada where field tomographic experiments were already carried out and documented by Paradis et al. (2016). Although aquifers are inherently heterogeneous in nature, using a homogeneous model eases the resolution comparison by isolating the effects of the spatial structure of hydraulic properties. The later has been already discussed by Paradis et al. (2015) for tomographic slug tests. For each of the two tomography experiments, we simulate 13 tests carried out in 0.61-m long stressed intervals located at different depths along the stressed well. For each test, hydraulic responses in the stressed interval itself and in 3 observation intervals (except for the uppermost and lowermost stressed intervals that use 2 observation intervals; see Figures 4a and 4b) distributed along the observation well are simultaneously recorded. A total of 13 stressed and 37 observation interval responses are thus available for the resolution analysis of each tomography experiment. As discussed later, both stressed and observation interval responses are needed in the analysis due to the non-applicability of the principle of reciprocity. Each slug test is initiated using an initial head of 4.5 m in the stressed interval. And, to fairly compare resolutions between slug tests and pumping tests, we calculate an equivalent pumping rate that produces a steady-state drawdown of 4.5 m in the stressed interval, which is identical to the initial head used for slug tests (Peres et al., 1989). For the present model this corresponds to a pumping rate of 4.0×10^{-5} m^3/s (2.4 LPM).

To compare the spatial resolution fields of the two tomography experiments, Figures 4a and 4b show the diagonal elements of the resolution matrix at the corresponding parameter grid cells for experiments with slug tests and pumping tests, respectively. Mean resolution values for cells within the inter-well region are also presented in Table 2 for this comparison. We note that this resolution analysis is based on the 10,000 s records of head or drawdown, which correspond to the termination of each slug test or to the time to reach steady-state conditions. Figures 4a and 4b thus show that independently of the test initiation method, resolutions for K_h, K_v/K_h and S_s are strongly focused on the stressed and observation wells with higher resolutions near the stressed well where sensitivities are larger. This agree with previous studies using both kind of tests (Vasco et al., 1997; Bohling, 2009; Paradis et al., 2015). Moreover, we see that resolution fields for K_h in Figures 4a and 4b are almost identical for the two experiments, as also expressed by similar mean resolution values (Experiments 1 and 2 in Table 2). Mean resolution values are also similar for K_v/K_h despite resolutions that appear much higher near the pumping well, whereas resolutions for S_s are definitely much lower for pumping than for slug tests.

Explanation of those similarities in parameter resolution can be found in Figures 5a, 5b and 5c. In Figure 5a, we plot as a reference the stressed interval responses for the equivalent slug and pumping tests, as previously discussed. In Figures 5b and 5c, we see that while drawdown due to pumping in the observation interval is three times larger than the head change induced by the slug test, the magnitude of the sensitivity for each hydraulic property is quite similar. Thus, assuming that correlation between sensitivity for each hydraulic property is almost identical for the two tests, comparable parameter resolutions are explained by the similarity in sensitivity magnitudes. Then, head changes due to slug tests are more efficient than drawdowns produced by pumping tests at resolving parameters, as head changes much lower than drawdowns produce similar sensitivity magnitudes. This is due to the sharper form of the head perturbation caused by the instantaneous slug of water applied in the stressed interval that produces larger spatial and temporal hydraulic gradients. Also, this explain why S_s is lower for pumping tests because temporal hydraulic gradients are smaller with pumping, which can be deduced from Figure 5c with S_s sensitivities for pumping about the third of the sensitivities for slug tests.

Table 2

Figure 4

Figure 5

4.2 Effect of reduced test stresses

In this section, we first illustrate the effects of reducing the pumping rate of each pumping test used for the tomography experiment. Indeed, as pumping tests use much more water than equivalent slug tests, such a reduction would be desirable at sites where the storage or injection of a large volume of water may be an issue (e.g., contaminated sites). For our previous tomography experiment, we used 9 L of water to initiate each slug test, whereas 400 L per pumping test was needed to reach steady-state conditions. We note that pneumatic slug test initiation method using air pressure to lower or raise the water level in the stressed interval could also be chosen to avoid using water at sensitive sites. Because a pumping test that would use only 9 L of water would produce non-significant drawdown in the observation intervals, we rather reduce pumping rates by four (experiment 4 in Table 2); thus 100 L of water is used instead of 400 L. We note that at this reduced rate, the peak head from the original slug test and steady-state drawdown of the 100 L pumping test recorded in the stressed intervals have the same magnitudes (Figure 6a).

As expected from the previous section, Figure 6b shows that reduced pumping rates decrease sensitivity magnitudes, which results in lower parameter resolutions as depicted in Table 2 (Experiment 4). Note that reducing initial heads by half leads to a similar decrease in resolutions for tomographic slug tests (Experiment 3 in Table 2). For those particular cases, the effect of reduced initial heads with respect to pumping rates is more pronounced (half the initial heads for a quarter of the original pumping rates) likely due to the head in the observation intervals that are closer to the level of noise, which increases parameter sensitivity correlations.

Figure 6

4.3 Effect of reduced test durations

In this section, we discuss the effects of reducing test durations of both slug tests and pumping tests in order to reduce data acquisition time of tomographic experiments that by design required numerous tests. For our previous synthetic experiment with pumping tests, each test in the field required as much as 2.75 h (10,000 s) to reach steady-state drawdown in the observation intervals. By considering that after each pumping test a recovery period equivalent to the pumping period is needed before conducting the next test, the 13 tests of this experiment would require more than 72 h of testing in the field. For those simulations, we consider recording head and drawdown for each test for a period of 1,000 s (17 min) instead of 10,000 s (2.75 h) (Figure 7a), which is considered more realistic for actual field applications.

As shown in Table 2 (Experiments 5 and 6), both experiments with slug tests and pumping tests see a reduction in resolutions. Examination of Figure 7b suggests that reduced test durations increase sensitivity correlations. In particular, we see that the sensitivity curves for K_v/K_h, and S_s of the pumping test are pretty similar for much of the duration of the test, which implies that their individual effect on drawdown cannot be resolved separately. Moreover, we see in Table 2 that the reduction in resolution is more severe with pumping because drawdown at 1,000 s are far from steady-state and still provide important information on parameters, whereas heads related to slug tests are close to their equilibrium state. Further reducing slug test durations long before heads reach their equilibrium state, at 400 s (7 min) for example (Experiment 7 in Table 2; Figures 7a and 7b), also reduces considerably resolutions to values close to pumping tests at 1,000 s. We note that pumping tests are longer due to wellbore storage that delays the aquifer response (see Figures 3c and 3d).

Figure 7

5 Summary and discussion

In this study, we assessed test initiation methods (slug and pumping tests) and some related field practices on parameter resolutions of tomography experiments. For this purpose, synthetic tomography experiments and their associated sensitivity matrices were generated using a radial flow model accounting for wellbore storage. The resolution analysis was based on a pseudo-inverse analysis of the sensitivity matrix with a noise level representative of field measurements. The main findings of this study are summarized and discussed below.

1. *Parameter resolutions are similar for tomography experiments using equivalent slug tests and pumping tests.* Using either slug tests or pumping tests that induce identical initial head and steady-state drawdown in the stressed interval lead to similar mean resolutions in hydraulic properties, except for S_s resolution that is slightly lower with pumping. Also, while there are slight differences, parameter resolution fields of tomography experiments simulated with a noise level representative of field conditions are essentially focused on the stressed and observation wells. Thus, for the two different test initiation methods, the same general limitations apply on the resolution of hydraulic properties because hydraulic tests are more sensitive to hydraulic properties in the immediate vicinity of the wells (Vasco et al., 1997).

2. *A slug test is more efficient at resolving parameters for the same magnitude in hydraulic perturbations induced in the observation intervals.* For instance, for the same values of head changes due to a slug test and drawdown induced by pumping in observation intervals, a slug test is more efficient at resolving parameters due to the sharper form of the induced head perturbation that produces larger sensitivities. So, in the field, one will try to maximize pumping rates even if the drawdown measured in the observation intervals appears "reasonably large". That could however be difficult as each pumping rate should be adjusted, generally by a trial-and-error process, according to the hydraulic properties surrounding the tested interval that can vary considerably for heterogeneous aquifer systems. In that respect, slug tests could be easier to perform because the initial head is set independently of the materials surrounding the well. However, large initial heads should be initiated in order to induce head changes in observation intervals that are larger than the noise level of the measurements, which may require a slightly more complex testing

equipment than a single pump (e.g., Paradis et al., 2016). Then, even if large head changes at a distance from a stressed well could be harder to produce with a slug test than drawdowns by pumping, the magnitude of the hydraulic perturbation alone is not a condition sufficient to assess the resolution potential of a tomographic experiment, and the sensitivities associated with each type of test should also be considered.

3. *Wellbore storage leads to the refutation of the principle of reciprocity for both slug tests and transient responses of pumping tests in wells with large diameters.* As a consequence of the non-applicability of the principle of reciprocity shown by synthetic experiments, the observation interval response does not provide a unique description of the heterogeneity because it is impossible to tell from this response whether the head change or the drawdown observed result from the flow rate induced by the test at the stressed interval, which is controlled by the surrounding heterogeneity, or the heterogeneity travelled by the hydraulic perturbation to the observation interval location. To obtain this information, stressed and observation interval responses for each test must be recorded in the field and used in the tomographic analysis to isolate the influence of the stressed interval response. Reciprocal tests using only observation interval responses could also be considered, but this alternative is less efficient as it requires twice the number of tests per tomographic experiment. From a practical perspective, head changes in stressed intervals caused by slug tests are generally easier to record with accuracy than drawdown due to pumping that are often influenced by pumping rate variations associated to the equipment itself. Large pumping rates can also induce important head losses in the stressed interval, which should be carefully considered in the analysis to avoid misinterpretation of the recorded water levels. Finally, it should be noted that using stressed and observation interval responses is also important to get better parameter resolutions as the different temporal sensitivity patterns for the different intervals contribute to decrease sensitivity correlations (Paradis et al., 2015).

4. *Reduced test durations produce lower resolutions regardless of the test initiation methods.* This finding implies that the recording of slug tests until heads have recovered their initial levels or pumping tests until steady-state is reached should be the preferred practice. However, this practice increases the overall acquisition time of tomography data. In this

regard, a slug test offers an important advantage over a pumping test for tomography experiments that generally need many tests since it requires less time per test. For the synthetic tomography experiments discussed in this paper, each slug test requires less than one-third of the time of a pumping test for the same hydrogeological conditions. Furthermore, since slug tests do not require a recovery period (heads are back to their initial levels) before testing the next interval as required after each pumping test, we estimate that an equivalent tomography experiment with slug tests is approximately seven times shorter to carry out in the field than an experiment with the same number of pumping tests.

Overall, this study demonstrates that tomographic slug tests are an interesting alternative to more commonly used tomographic pumping tests. Indeed, the same level of parameter resolutions could be achieved for a much shorter field effort. This means, that this could foster the use of hydraulic tomography by a larger community of scientists or practitioners outside of the current research community. For future work it would be interesting to assess resolutions and field-efficiency of periodic pumping tests and slug tests as proposed by Cardiff et al. (2013) and Guiltinan and Becker (2015), respectively.

6 Acknowledgements

This study was supported by the Geological Survey of Canada as part of the Groundwater Geoscience Program and by NSERC Discovery Grants held by R.L. and E.G. The authors would like to thank the four anonymous reviewers that provided constructive reviews. This is ESS contribution number 20150440.

7 References

Aster R C, Borchers B, Thurber C H (2005) Parameter Estimation and Inverse Problems. 301pp Elsevier Amsterdam

Berg S J, Illman W A (2011) Three-dimensional transient hydraulic tomography in a highly heterogeneous glaciofluvial aquifer-aquitard system. Water Resour Res 47:W10507 doi: 10.1029/2011WR010616

Berg S J, Illman W A (2013) Field study of subsurface heterogeneity with steady state hydraulic tomography. Groundwater 51(1):29-40 doi:10.1111/j.1745–6584.2012.00914.x

Berg S J, Illman W A (2015) Comparison of hydraulic tomography with traditional methods at a highly heterogeneous site. Groundwater 53(1):71-89 doi:10.1111/gwat.12159

Bohling G C (2009) Sensitivity and resolution of tomographic pumping tests in an alluvial aquifer. Water Resour Res 45: W02420, 10.1029/2008WR007249

Bohling G C, Butler Jr J J (2001) Lr2dinv: A finite-difference model for inverse analysis of two-dimensional linear or radial groundwater flow. Comput Geosci 27:1147-1156

Bohling G C, Butler Jr J J (2010) Inherent limitations of hydraulic tomography. Ground Water 48:809-824 doi:10.1111/j.1745-6584.2010.00757.x

Bohling G C, Butler Jr J J, Zhan X, Knoll M D (2007) A Field Assessment of the value of steady-shape hydraulic tomography for characterization of aquifer heterogeneities. Water Resour Res 43(5) W05430 : doi:10.1029/2006WR004932

Bohling G C, Zhan X, Butler Jr J J, Zheng L (2002) Steady shape analysis of tomographic pumping tests for characterization of aquifer heterogeneities. Water Resour Res 38(12) 1324:doi:10.1029/2001WR001176

Butler Jr J J, McElwee C D, Bohling G C (1999) Pumping tests in networks of multilevel sampling wells: Motivation and methodology. Water Resour Res 35(11):3553-3560 doi:10.1029/1999WR900231

Brauchler R, Liedl R, Dietrich P (2003) A travel time based hydraulic tomographic approach. Water Resour Res 39(12) 1370 doi: 10.1029/2003WR002262

Brauchler R, Hu R, Vogt T, Al-Halbouni D, Heinrichs T, Ptak T, Sauter M (2010) Cross-well slug interference tests: An effective characterization method for resolving aquifer heterogeneity. J Hydrol 384(1-2):33-45

Brauchler, R.; Hu, R.; Dietrich, P.; et al. (2011) A field assessment of high-resolution aquifer characterization based on hydraulic travel time and hydraulic attenuation tomography. Water Resour Res 47 W03503

Brauchler R, Hu R, Hu L, Jiménez S, Bayer P. Dietrich P, Ptak T (2013) Rapid field application of hydraulic tomography for resolving aquifer heterogeneity in unconsolidated sediments Water Resour Res 49(4):2013-2024

Butler Jr J J (2005) Hydrogeological methods for estimation of hydraulic conductivity. Edited by Y Rubin Y, Hubbard S in Hydrogeophysics pp 23-58 Springer New York

Butler Jr J J, McElwee C D (1990) Variable-rate pumping tests for radially symmetric nonuniform aquifers. Water Resour Res 26(2):291-306

Butler Jr J J, McElwee C D (1995) Well-testing methodology for characterizing heterogeneities in alluvial-aquifer systems: Final technical report. Kans Geol Surv Open File Report no 75-95

Caers J (2005) Petroleum Geostatistics. 88 p Soc of Pet Eng, Richardson, Tex

Cardiff M, Barrash W (2011) 3-D transient hydraulic tomography in unconfined aquifers with fast drainage response. Water Resour Res 47:W12518 doi:10.1029/2010WR010367

Cardiff M, Barrash W, Kitanidis P K (2012) A field proof-of-concept of aquifer imaging using 3-D transient hydraulic tomography with modular, temporarily-emplaced equipment. Water Resour Res 48:W05531 doi:10.1029/2011WR011704

Cardiff M, Bakhos T, Kitanidis P K, Barrash W (2013) Aquifer heterogeneity characterization with oscillatory pumping: Sensitivity analysis and imaging potential. Water Resour Res 49(9):5395-5410

Cardiff M, Barrash W, Kitanidis P K, Malama B, Revil A, Straface S, Rizzo E (2009) A potential-based inversion of unconfined steady-state hydraulic tomography. Ground Water 47(2):259-270 doi:10.1111/j.1745–6584.2008.00541.x

Carrera J, Neuman S P (1986) Estimation of aquifer parameters under transient and steady state conditions: 1. Maximum likelihood method incorporating prior information. Water Resour Res 22(2):199-210 doi:10.1029/WR022i002p00199

Carrera J, Alcolea A, Medina A, Hidalgo J, Slooten L J (2005) Inverse problem in hydrogeology. Hydrogeol J 13:206-222 doi: 10.1007/s10040-004-0404-7

Clemo T, Michaels P, Lehman R M (2003) Transmissivity resolution obtained from the inversion of transient and pseudo-steady drawdown measurements. in Proceedings of MODFLOW and More 2003 Understanding Through Modeling p 629-633, Int Ground Water Model Cent, Golden CO USA

Doherty J (2003) Ground water model calibration using pilot points and regularization. Ground Water 41(2) :170-177 doi:10.1111/j.1745– 6584.2003.tb02580.x

Dougherty D E, Babu D K (1984) Flow to a Partially Penetrating Well in a Double-Porosity Reservoir. Water Resour Res 20(8):1116-1122 doi:10.1029/WR020i008p01116

Ferris J G, Knowles D B (1963) The slug-injection test for estimating the coefficient of transmissibility of an aquifer. In: US Geological Survey Water-Supply Paper 15361-I, R. Bentall (compiler), p. 299.

Fienen M N, Clemo T, Kitanids P K (2008) An interactive Bayesian geostatistical inverse protocol for hydraulic tomography. Water Resour Res 44:W00B01 doi:10.1029/2007WR006730

Guiltinan E, Becker M W (2015) Measuring well hydraulic connectivity in fractured bedrock using periodic slug tests. J Hydrol 521 :100-107 doi: 10.1016/j.jhydrol.2014.11.066

Gottlieb J, Dietrich P (1995) Identification of the permeability distribution in soil by hydraulic tomography. Inverse Probl 11:353-360 doi:10.1088/0266–5611/11/2/005

Huang, S.-Y., J.-C. Wen, T.-C. J. Yeh, W. Lu, H.-L. Juan, C.-M. Tseng, J.-H. Lee, and K.-C. Chang S Y (2011) Robustness of joint interpretation of sequential pumping tests: Numerical and field experiments. Water Resour Res 47:W10530, doi:10.1029/ 2011WR010698

Illman W A, Craig A J, Liu X (2008) Practical issues in imaging hydraulic conductivity through hydraulic tomography. Ground Water 46(1) :120-132 doi:10.1111/j.1745-6584.2007.00374.x.

Illman W A, Liu X, Craig A (2007) Steady-state hydraulic tomography in a laboratory aquifer with deterministic heterogeneity: Multimethod and multiscale validation of hydraulic conductivity tomograms. J Hydrol 341(3-4) :222-234 doi:10.1016/j.jhydrol.2007.05.011

Illman W A, Liu X, Takeuchi S, Yeh T J, Ando K, Saegusa H (2009) Hydraulic tomography in fractured granite: Mizunami underground research site, Japan. Water Resour Res 45:W01406 doi:10.1029/2007WR006715

Kitanidis, P K (1995) Quasi-linear geostatistical theory for inversing. Water Resour Res 31(10): 2411–2419

Kruseman G P, de Ridder N A (2000) Analysis and evaluation of pumping test data. ILRI Publishing Netherlands 377pp

Leven C, Dietrich P (2006) What information we get from pumping tests? Comparing pumping configurations using sensitivity coefficients. J Hydrol 319:199-215

Liu, X, Kitanidis P K (2011) Large-scale inverse modeling with an application in hydraulic tomography. Water Resour Res 47 W02501 doi:10.1029/2010WR009144

McElwee C D, Yukler M A (1978) Sensitivity of groundwater models with respect to variations in transmissivity and storage. Water Resour Res 14(3):451-459 doi:10.1029/WR014i003p00451

McKinley R M, Vela S, Carlton L A (1968), A field application of pulse-testing for detailed reservoir description. J Petrol Tech 20(3):313-321

Menke W (2012) Geophysical Data Analysis: Discrete Inverse Theory. 3rd ed. 293pp Academic Press

Moore E H (1920) On the reciprocal of the general algebraic matrix. Bull Am Math Soc 26:394-395

Novakowski K S (1989) Analysis of pulse interference tests. Water Resour Res 25(11):2377-2387

Oliver D S (1993) The influence of nonuniform transmissivity and storativity on drawdown. Water Resour Res 29(1):169-178

Paradis D, Gloaguen E, Lefebvre R, Giroux B (2015) Resolution analysis of tomographic slug tests head data: Two-dimensional radial case. Water Resour Res 51:2356-2376 doi:10.1002/2013WR014785

Paradis, D., E. Gloaguen, R. Lefebvre, and B. Giroux (2016) A field proof-of-concept of tomographic slug tests in an anisotropic littoral aquifer. J Hydrol 536:61-73 http://dx.doi.org/10.1016/j.jhydrol.2016.02.041

Penrose, R (1955) A generalized inverse for matrices. Proc Cambridge Philos Soc 51:406-413

Peres, A M, Onur M, Reynolds A C (1989) A new analysis procedure for determining aquifer properties from slug test data. Water Resour Res 25(7):1591-1602

Rovey C W, Cherkauer II D S (1995) Scale dependency of hydraulic conductivity measurements. Ground Water 33(5):769-780

Rubin, Y, Hubbard S S (2005) Hydrogeophysics. 523 p Springer, Dordrecht, Netherlands

Sageev, A (1986) Slug test analysis. Water Resour Res 22(8):1323-1333

Soueid Ahmed, S A, Jardani, A, Revil A. Dupont J P (2014) Hydraulic conductivity field characterization from the joint inversion of hydraulic heads and self-potential data. Water Resour Res 50:3502-3522 doi:10.1002/2013WR014645

Sun R, Yeh T-C J, Mao D, Jin M, Lu W, Hao Y (2013) A temporal sampling strategy for hydraulic tomography analysis. Water Resour Res 49:3881-3896 doi:10.1002/wrcr.20337

Tikhonov, A N (1963) Regularization of incorrectly posed problems. Sov Math Dokl 4(6):1624-1627

Tikhonov, A N, Arsenin V A (1977) Solution of Ill-Posed Problems. 258 p., John Wiley New-York

Tonkin, M J, Doherty J (2005) A hybrid regularization methodology for highly parameterized environmental models. Water Resour Res 41 W10412 doi:10.1029/2005WR003995

Tosaka H, Masumoto K, Kojima K (1993) Hydropulse tomography for identifying 3-D permeability distribution in high level radioactive waste management. Proceedings of the Fourth Annual International Conference of the ASCE, pp. 955-959, Am. Soc. Civ. Eng., Reston, Va.

Vasco D W, Datta-Gupta A, Long J C S (1997) Resolution and uncertainty in hydrologic characterization. Water Resour Res 33(3):379-397 doi:10.1029/96WR03301

Xiang, J, Yeh T-C J, Lee C-H, Hsu K-C, Wen J-C (2009) A simultaneous successive linear estimator and a guide for hydraulic tomography analysis. Water Resour Res 45 W02432 doi:10.1029/2008WR007180

Yeh T-C J, Liu S (2000) Hydraulic tomography: Development of a new aquifer test method. Water Resour Res 36 (8):2095-2105 doi:10.1029/2000WR900114

Zha, Y, Yeh T-C J, Mao D, Yang J, Lu W (2014) Usefulness of flux measurements during hydraulic tomographic survey for mapping hydraulic conductivity distribution in a fractured medium. Adv Water Resour 71:162-176 doi:10.1016/j.advwatres.2014.06.008

Zhu J, Yeh T-C J (2005) Characterization of aquifer heterogeneity using transient hydraulic tomography. Water Resour Res 41:W07028 doi:10.1029/2004WR003790

Figures Captions

Figure 1. Schematic diagram illustrating the general approach used for the evaluation of the resolution matrix of a tomography experiment. 1) Starting from an idealized aquifer system and a test configuration, sensitivities are calculated using the numerical flow simulator through a perturbation approach. 2) A Moore-Penrose pseudo-inverse approach is then applied on the resulting sensitivity matrix to evaluate the associated resolution matrix. 3) Resolution characteristics of the tomography experiment is finally analyzed through inspection of the diagonal elements of the resolution matrix.

Figure 2. Head and drawdown for reciprocal slug tests and pumping tests, respectively, for the case with a test configuration symmetrical with respect to layering in K_h, K_v and S_s. (a) Aquifer model and test configuration; (b) Head for reciprocal slug tests; (c) Drawdown for reciprocal pumping tests considering wellbore storage in the stressed well; and (d) Drawdown for reciprocal pumping tests neglecting wellbore storage in the stressed interval. Note that reciprocal tests are simulated by mirroring the vertical locations of the stressed and observation intervals to represent the two different testing directions. Values of K_h, K_v and S_s for the different simulations are compiled in Table 1.

Figure 3. Head and drawdown for reciprocal slug tests and pumping tests, respectively, for the case with a test configuration asymmetrical with respect to layering in K_h, K_v and S_s. (a) Aquifer model and test configuration; (b) Head for reciprocal slug tests; (c) Drawdown for reciprocal pumping tests considering wellbore storage in the stressed well; and (d) Drawdown for reciprocal pumping tests neglecting wellbore storage in the stressed interval. Note that reciprocal tests are simulated by mirroring the vertical locations of the stressed and observation intervals to represent the two different testing directions. Values of K_h, K_v and S_s for the different simulations are compiled in Table 1.

Figure 4. Diagonal elements of the resolution matrix for K_h, K_v/K_h, and S_s associated with the analysis of the synthetic 10,000 s head (a) and drawdown (b) records for a homogeneous and anisotropic model. Resolutions are based on a Moore-Penrose pseudo-inverse of the sensitivity

matrix for a relative parameter error of 10% and a random noise with a standard deviation of $2x10^{-4}$ m (see Supplementary Material for supportive information).

Figure 5. Head and drawdown in (a) stressed and (b) observation intervals for a single test. Sensitivities in K_h, K_v/K_h, and S_s for the observation interval in (c) are computed for the entire inter-well region. Stressed and observation intervals are located in the middle of the wells.

Figure 6. (a) Head and drawdown as well as (b) sensitivities in K_h, K_v/K_h, and S_s for the observation interval of a single test considering a reduced pumping rate of $1.0x10^{-5}$ m^3/s (0.6 LPM). Head and sensitivities for the slug test in gray are from Figure 5 for reference. Head and sensitivities for reduced initial slug test head of 2.25 m (Table 2) are not shown, but their magnitudes are half those of Figure 5 (gray lines).

Figure 7. (a) Head and drawdown as well as (b) sensitivities in K_h, K_v/K_h, and S_s for the observation interval of a single test considering a reduced test duration lasting 1,000 s instead of 10,000 s.

Figure 1

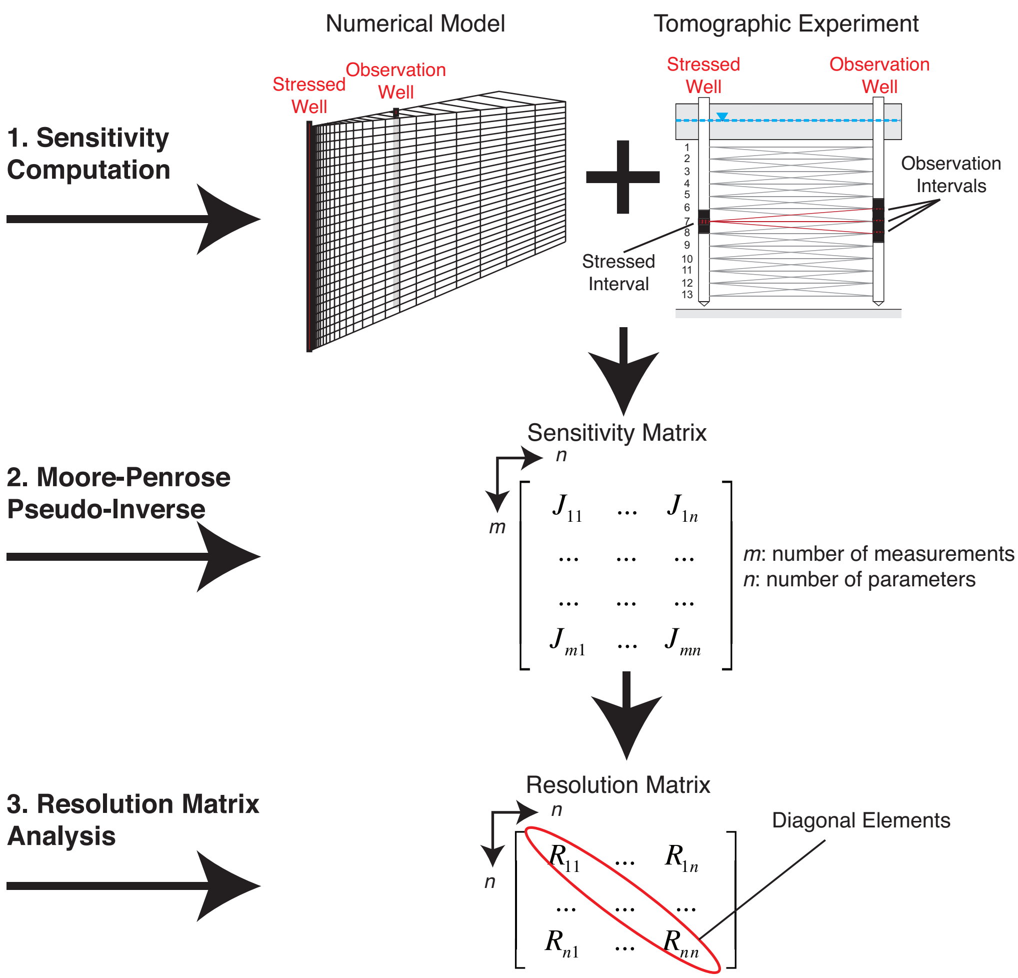

Numerical Model
Tomographic Experiment
Stressed Well
Observation Well
Stressed Well
Observation Well
1. Sensitivity Computation
Observation Intervals
Stressed Interval
1
2
3
4
5
6
7
8
9
10
11
12
13
Sensitivity Matrix
2. Moore-Penrose Pseudo-Inverse
n
m
J11 ... J1n
... ...
... ...
Jm1 ... Jmn
m: number of measurements
n: number of parameters
Resolution Matrix
3. Resolution Matrix Analysis
Diagonal Elements
n
n
R11 ... R1n
... ...
Rn1 ... Rnn

Figure 2 corrected

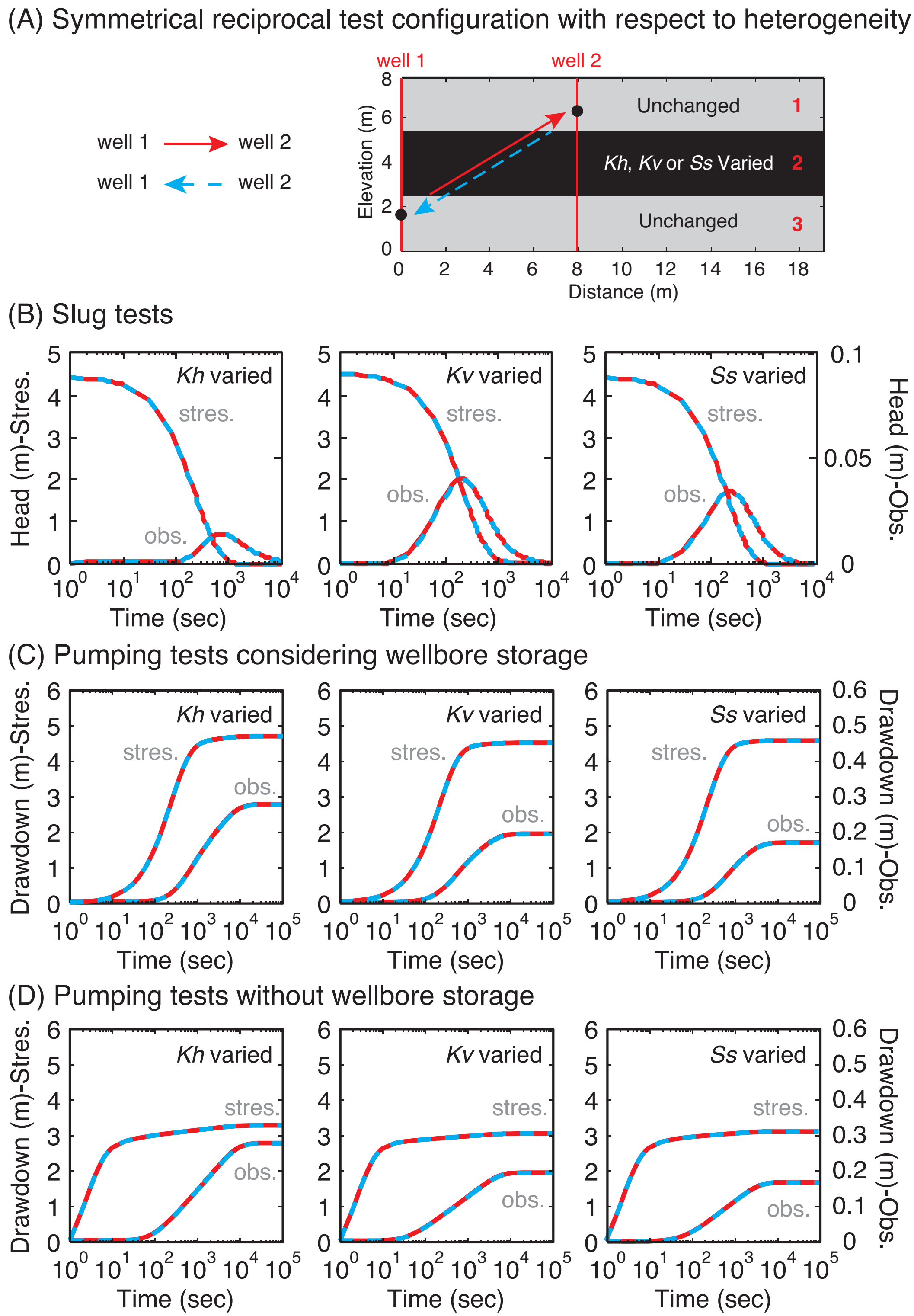

Figure 3 modified

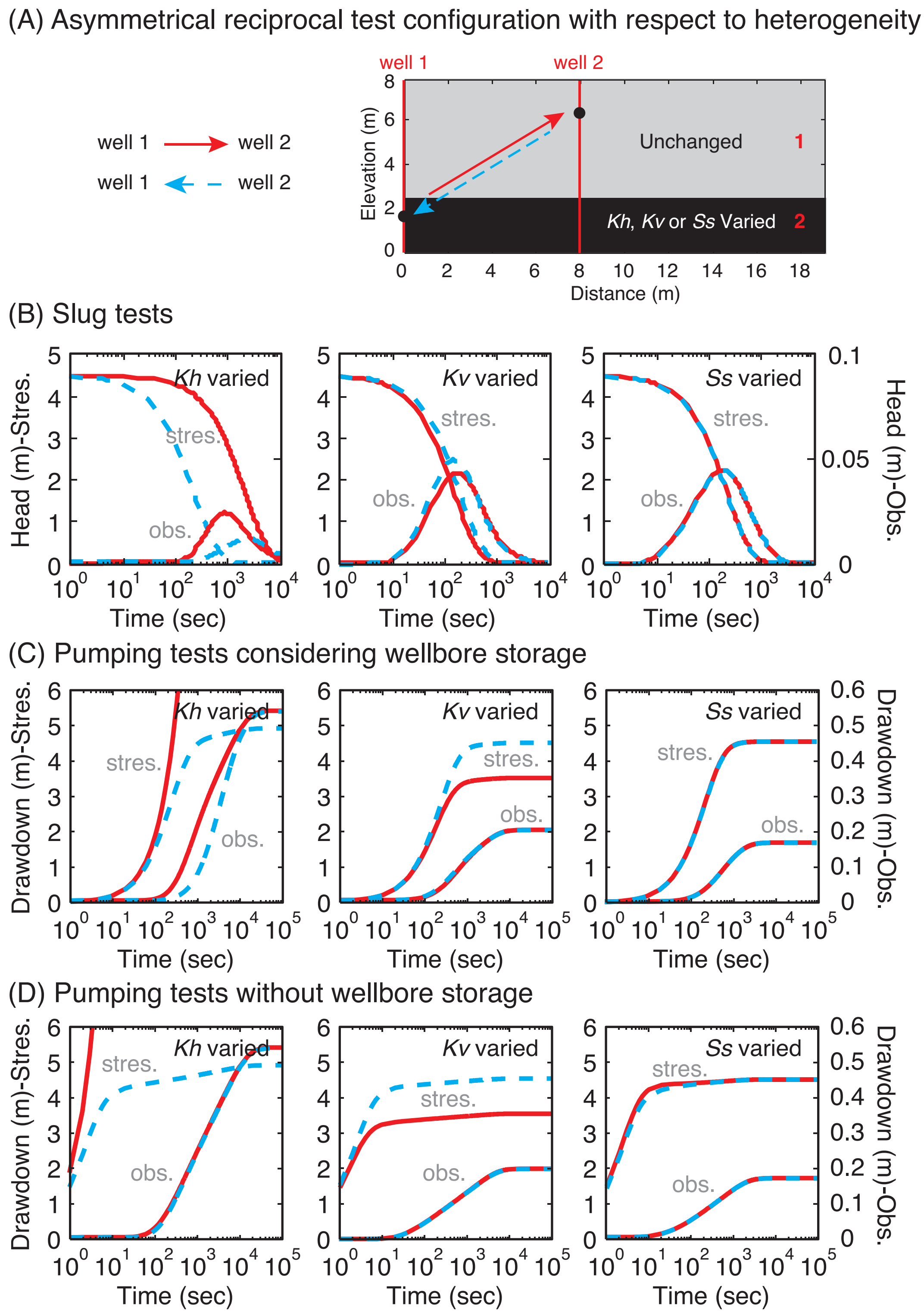

Figure 4

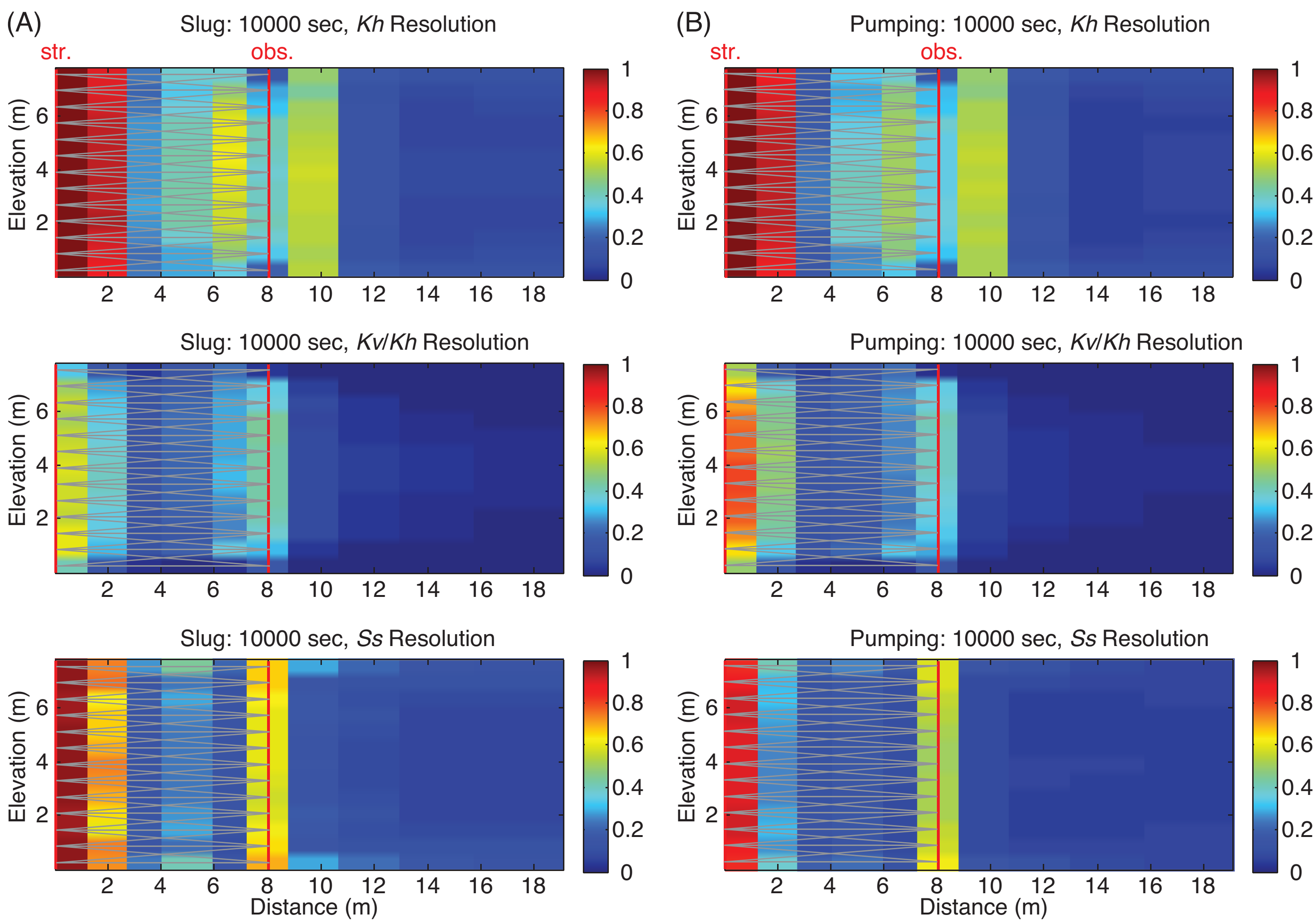

(A)
Slug: 10000 sec, Kh Resolution
str.
obs.
Slug: 10000 sec, Kv/Kh Resolution
Slug: 10000 sec, Ss Resolution
Elevation (m)
Distance (m)
(B)
Pumping: 10000 sec, Kh Resolution
Pumping: 10000 sec, Kv/Kh Resolution
Pumping: 10000 sec, Ss Resolution

Figure 5

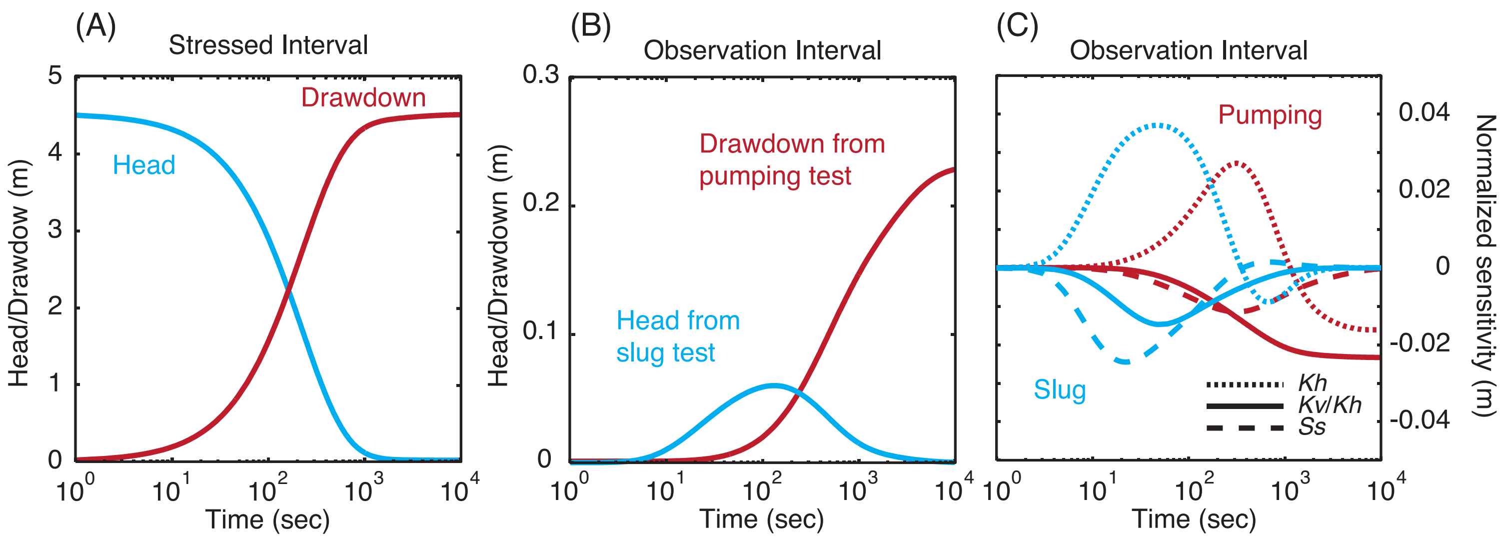

(A)
Stressed Interval
Head
Drawdown
Head/Drawdow (m)
Time (sec)
(B)
Observation Interval
Drawdown from
pumping test
Head from
slug test
Head/Drawdown (m)
Time (sec)
(C)
Observation Interval
Pumping
Slug
Kh
Kv/Kh
Ss
Normalized sensitivity (m)
Time (sec)

Figure 6

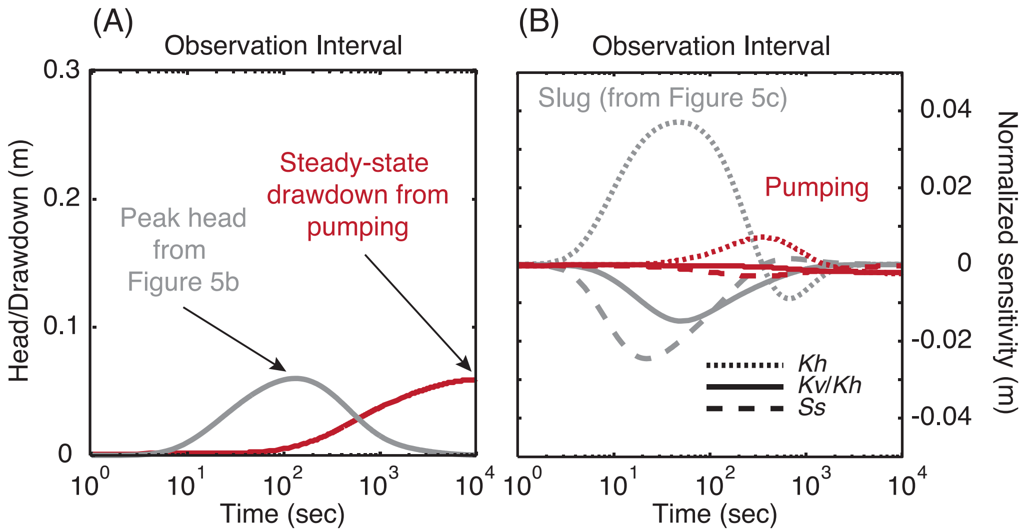

(A)
Observation Interval
0.3
0.2
0.1
0
Head/Drawdown (m)
Peak head from Figure 5b
Steady-state drawdown from pumping
10^0
10^1
10^2
10^3
10^4
Time (sec)
(B)
Observation Interval
Slug (from Figure 5c)
Pumping
0.04
0.02
0
-0.02
-0.04
Normalized sensitivity (m)
Kh
Kv/Kh
Ss
10^0
10^1
10^2
10^3
10^4
Time (sec)

Figure 7

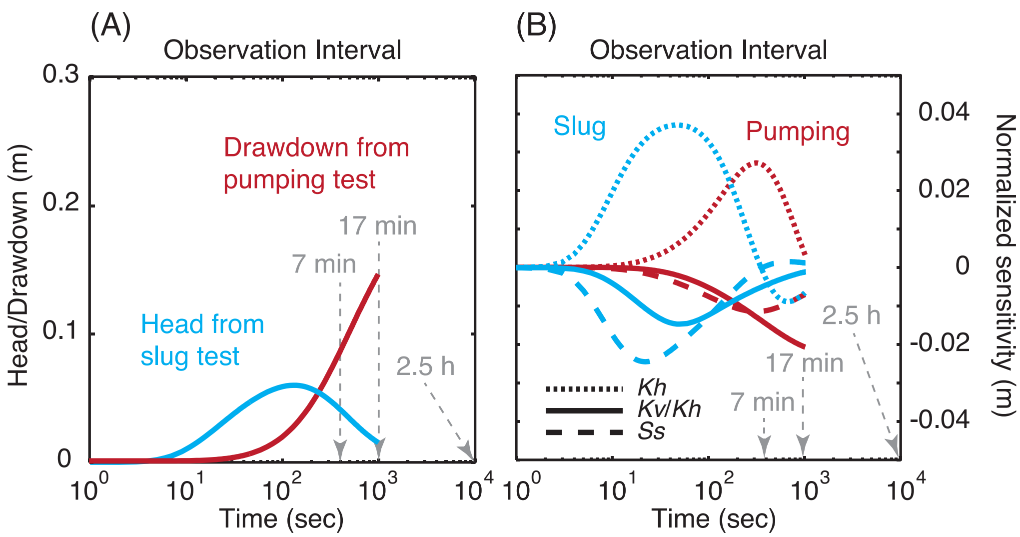
(A)
Observation Interval
Head/Drawdown (m)
Drawdown from
pumping test
Head from
slug test
17 min
7 min
2.5 h
Time (sec)
(B)
Observation Interval
Slug
Pumping
Normalized sensitivity (m)
Kh
Kv/Kh
Ss
17 min
7 min
2.5 h
Time (sec)

Table 1. Hydraulic properties of each layer in the model used for the verification of the principle of reciprocity for slug tests and pumping tests.

Simulation	Layer	K_h (ms^{-1})	K_v (ms^{-1})	S_s (m^{-1})
K_h varied	2	$1x10^{-6}$	$1x10^{-6}$	$1x10^{-5}$
K_v varied	2	$1x10^{-5}$	$1x10^{-5}$	$1x10^{-5}$
S_s varied	2	$1x10^{-5}$	$1x10^{-6}$	$1x10^{-6}$
For all simulations	1 and 3	$1x10^{-5}$	$1x10^{-6}$	$1x10^{-5}$

Table 2. Mean resolution for cells within the inter-well region for different tomography experiments using different test initiation methods (slug and pumping), test durations and pumping rates.

Experiment	**Test Duration (s)**	**Initial Head (m)**	**Pumping Rate (x10^{-5} m^3/s)**	**Mean Resolution for Inter-Well Region**		
				K_h (ms^{-1})	**K_v/K_h (-)**	**S_s (m^{-1})**
1.Slug tests	10,000	4.5	-	0.57	0.30	0.48
2.Pumping tests	10,000	-	4.0	0.54	0.33	0.36
3.Reduced initial slug test heads	10,000	2.25	-	0.52	0.24	0.36
4.Reduced pumping rates	10,000	-	1.0	0.49	0.23	0.26
5.Reduced slug test durations	1,000	4.5	-	0.50	0.24	0.37
6.Reduced pumping test durations	1,000	-	4.0	0.41	0.21	0.21
7.Reduced slug test durations	400	4.5	-	0.41	0.20	0.24